Lifetime deflections of long-span bridges under dynamic and growing traffic load

Naiwei Lu [1]; Michael Beer [2]; Mohammad Noori [3]; Yang Liu [4]

Abstract:

Steady traffic growth may pose a safety hazard to in-service bridges, especially long-span bridges subjected to the simultaneous presence of multiple heavy-duty trucks. This study presents a methodology for evaluating the statistical extrapolation of traffic load effects on long-span bridges. As part of the contributions advancing the state of the art, this study addresses several challenging issues, including traffic growth, the resulting dynamic impact and actual traffic patterns. The nonstationarity of the traffic load effects due to traffic growth is considered in a series system compounded by several interval traffic models. The dynamic impacts of traffic loads are simulated by a traffic-bridge coupled vibration system, and its statistical characteristics are captured using the Rice level-crossing model. The actual traffic pattern is simulated by stochastic traffic flows based on the statistics of the weigh-in-motion measurements of a highway bridge. Two numerical examples demonstrate the ability of the interval traffic growth model to capture the nonstationarity of the growing traffic loads. In

[1] Lecturer, School of Civil Engineering and Architecture, Changsha Univ. of Science and Technology, Changsha Hunan 410114, China. (Corresponding author). Email: lunaiweide@163.com; formerly, Postdoctoral Research Fellow, International Institute for Urban Systems Engineering, Southeast Univ., Nanjing Jiangsu 210096, China

[2] Professor, Institute for Risk and Reliability, Leibniz Univ. Hannover, Hannover 31509, Germany. Email: beer@irz.uni-hannover.de

[3] Professor, Dept. of Mechanical Engineering, California Polytechnic State Univ., San Luis Obispo, CA 93407, USA, and Affiliate Distinguished Professor, International Institute for Urban Systems Engineering, Southeast Univ., Nanjing Jiangsu 210096, China Email: contact@mohammadnoori.com

[4] Professor, School of Civil Engineering and Architecture, Changsha Univ. of Science and Technology, Changsha Hunan 410114, China. Email: liuyangbridge@163.com

addition, a case study of a long-span suspension bridge shows the effectiveness of implementing the proposed methodology for the statistical extrapolation of the maximum deflection. The numerical results of the case study demonstrate that the degradation of the road roughness conditions leads to more level crossings, but results in a slight increase in the extrapolation of the deflection. However, the traffic growth results in rapid increases in both the extrapolated deflection and the probability of exceedance of the deflection limit.

Keywords:

Long-span bridge; Traffic load; Deflection; Vehicle-bridge interaction; Level-crossing; Road roughness condition; Traffic growth

Introduction

Due to the intense competition in transportation of goods in the global market, truck overloading has increased and has led to the collapse of numerous in-service highway bridges over the last few decades (Fu et al. 2009; Zhu et al. 2010). A steady growth in traffic volume and vehicle weight may pose safety hazards to in-service bridges (Deng et al. 2016; Wang et al. 2017). Although the live-load model in a design specification has a confidence level that ensures the bridge safety over the expected lifetime, such levels may be underestimated relative to actual traffic loading scenarios involving extremely overloaded trucks. For instance, a case study conducted by Han et al. (2015) showed that 4 of 1319 trucks yielded bridge hogging moments larger than the value estimated by China's designed live-load model. In addition to the general phenomenon of traffic loading, long-span bridges are flexible and ductile, especially in the event of the simultaneous presence of multiple heavy-duty trucks (Zhou and Chen 2014). To ensure the serviceability of long-span bridges, design specifications have recommended certain deflection limits, such as $L/250$ and $L/300$ for the maximum deflection and the maximum deflection range in the Eurocode 3 (ECS 2005), where

41 L is the effective length of a bridge. Therefore, the lifetime deflection and the reliability
42 calibration of long-span bridges considering the actual traffic load are worth investigating.
43 Implementations of site-specific measurements in bridge engineering have been
44 investigated by numerous studies, such as the calibration of design live-load models (Nowak,
45 1995; Kwon et al. 2011; Enright et al. 2013), bridge fatigue reliability assessment (Lu et al.
46 2016) and the characteristic traffic load effect extrapolation (Oconnor, 2005; Caprani 2008;
47 OBrien and Engright 2011). Conventional methods for extrapolating traffic load effects are
48 associated with the generalized extreme value (GEV) theory and Rice's level-crossing theory
49 (OBrien et al. 2015b). Nonstationary traffic load effects on short-span bridges (L<30 m) due
50 to traffic growth has been investigated by OBrien et al. (2014). In addition to investigations
51 on the static extrapolation cited above, studies on dynamic extrapolation of the traffic load
52 effects have been conducted. For instance, OBrien et al. (2010) presented an assessment
53 dynamic ratio (ADR) to investigate the influence of vehicle-bridge interaction (VBI) on
54 medium-span bridges. Subsequently, Caprani et al. (2012) utilized the ADR in conjunction
55 with a multivariate GEV theory to investigate the dynamic allowance of a highway bridge
56 under long-term traffic loading. Even though these developments are mostly concentrated on
57 short- to medium-span bridges, a solid foundation has been provided for the extended
58 application to long-span bridges.
59 The simultaneous presence of multiple trucks increases the complexity of the statistical
60 extrapolation for a long-span bridge based on the actual traffic pattern. The traffic load effect
61 under individual truck loads can be treated following an independent identical distribution
62 (IID), but the load effect induced by the presence of multiple vehicles violates the IID
63 assumption. To solve this problem, Caprani et al. (2008) presented a maximum traffic loading
64 event accounting for the simultaneous presence of multiple trucks to evaluate the maximum
65 traffic load effect. Critical traffic loading scenarios on long-span bridges were presented by

66 OBrien et al. (2012) utilizing microscale stochastic traffic flows simulated based on weigh-in-
67 motion (WIM) data. Lifetime traffic loading scenarios on medium span bridges were modeled
68 by Enright and OBrien (2013) with the consideration of free-flowing traffic conditions.
69 Several recent studies have emphasized the traffic loading behavior on long-span bridges. For
70 instance, OBrien et al. (2015a) utilized a microscale traffic model to investigate congested
71 traffic loading on long-span bridges with consideration of truck proportions. In this scenario,
72 slow-moving traffic led to greater loading than fully stopped traffic. Caprani et al. (2016)
73 investigated the influence of microscale traffic scenarios on the extrapolated results. Ruan et
74 al. (2016) used site-specific WIM data to estimate the traffic load effect of a multi-pylon
75 cable-stayed bridge and the maximum static friction coefficient of an anti-sliding model for a
76 suspension bridge. The dynamic effects of traffic loading due to deteriorated road surfaces on
77 long-span bridges lead to higher dynamic amplification factors (DAFs) (Chen and Wu 2010).
78 The studies cited above contributed to the understanding of the statistical extrapolation of the
79 traffic load effects on long-span bridges.

80 In practice, stochastic traffic flow models are an effective and realistic and need to be
81 considered especially for probabilistic applications of long-span bridges during multiple-truck
82 events. Since a bridge lifetime is much longer than the duration of the recorded traffic data,
83 some conventional assumptions in this field might be inappropriate. First, the traffic volume
84 will grow during the lifetime of a bridge, leading to virtual nonstationarity of traffic load
85 effects over the bridge lifetime. This phenomenon apparently violates the stationarity
86 assumption in the GEV theory. Consequently, even though the dynamic effects of traffic
87 loading are not significant for flexible long-span bridges, the deterioration of the road surface
88 will amplify the traffic load effect. These issues increase the complexity of the probabilistic
89 investigation of the traffic load effects. However, to the best of the authors' knowledge, the
90 influence of some actual traffic load behaviors, such as dynamic effects and traffic growth, on

the statistical extrapolation for long-span bridges remains unclear.

This study aims to present a methodology for the statistical extrapolation of traffic load effects on long-span bridges considering several challenging factors, including traffic growth, dynamic impacts and actual traffic patterns. The actual traffic pattern is simulated via stochastic traffic flows based on the statistics of WIM measurements of a highway bridge. The nonstationary traffic load effects due to traffic growth are considered in a series system composed of several interval traffic models. The traffic dynamic impact is simulated by a traffic-bridge coupled vibration system and its statistical characteristics are captured using Rice level-crossing model. The proposed methodology is demonstrated and verified via two numerical examples and subsequently applied to a case study of a suspension bridge. The effects of road surface deterioration and traffic growth on the statistical extrapolation of the maximum deflection and the probability of exceedance of the deflection limit are investigated.

Theoretical bases of Rice extrapolation for traffic-bridge interaction

The traffic dynamic effects on bridges due to traffic-bridge interaction impacts the statistical extrapolation. To investigate the differences between the static and dynamic extrapolations, Rice formula is utilized to count the number of level crossings to capture the difference in the probabilistic models. Herein, the theoretical formulations of the traffic-bridge interaction and Rice formula are introduced.

Traffic-bridge interaction

The traffic-bridge interaction comes from the VBI that is conventionally used for DAF estimation. In a VBI system, the vehicle is usually simulated by the degrees of freedom (DOFs) in physical coordinates. For instance, a 3D 2-axle truck model as shown in **Figs. 1** can be simulated by 7 DOFs including two rotational (θ_{r1} and θ_{r2}) and a vertical translational

115 motions (Z_{vb}) of the vehicle rigid body, as well as vertical translational motions (Z_{aL}^{1}, Z_{aR}^{1},

116 Z_{aL}^{2}, Z_{aR}^{2}) of each vehicle wheel, where K_{vuL}^{i}, K_{vlR}^{i}, C_{vuL}^{i} and C_{vlR}^{i} are the stiffness and the

117 damping terms of the upper and lower suspension system on the left and right wheels,

118 respectively. The equation for the motions in the VBI system can be solved by a modal

119 superposition approach or a step-by-step integration approach in the time domain (Zhang and

120 Xia 2013).

121 The simultaneous presence of multiple vehicles is unique to long-span bridges

122 compared with short-span bridges. Initially, investigations (Cai and Chen, 2004; Chen and

123 Cai, 2007) suggested that the interaction effects between multiple vehicles on a flexible long-

124 span bridge were insignificant. Subsequently, the up-to-date researches (Zhou and Chen 2015;

125 Chou and Chen 2016) found that interaction effects exist in traffic flows with multiple

126 presences of vehicles in motion. This study utilizes the equivalent dynamic wheel load

127 (EDWL) approach proposed by Chen and Wu (2010) to evaluate the dynamic traffic-flow

128 load effects. The EDWL approach utilizes time-variant forces accounting for the mode shapes

129 and natural frequencies of the bridge to approximate the VBI forces. Eventually, the

130 cumulative EDWL acting on the bridge can be defined as follows:

131 $$\{F(t)\}_{eq}^{wheel} = \sum_{j=1}^{n_v}\left\{\left[1 - EDWL_j(t)/G_j\right]G_j \cdot \sum_{k=1}^{n_a}\left\{h_k[x_j(t) + \alpha_k[x_j(t)d_j(t)]]\right\}\right\} \quad (1a)$$

132 $$EDWL = \sum_{i=1}^{n}\left(K_{vl}^{i}\overline{Z}_a^i + C_{vl}^{i}\overline{\dot{Z}}_a^i\right) \quad (1b)$$

133 where $EDWL_j(t)$ is the dynamic load of the j-th vehicle at time t; G_j, x_j, and d_j are the weight,

134 longitudinal location, and transversal location of the center of gravity of the jth vehicle on the

135 bridge, respectively; h_k and a_k are the vertical and torsional mode shapes for the kth mode of

136 the bridge, respectively; n_v and n_a are the number of vehicles on the bridge and the number of

137 axles of the j-th vehicle, respectively; and $\overline{Z}_a^i$ and $\overline{\dot{Z}}_a^i$ are the relative vertical displacement

and velocity of the wheel axle with respect to the bridge, respectively. The number of vehicles on the bridge changes with time depending on the stochastic traffic flow, and the road-roughness coefficient (RRC) is considered in the vertical displacement and velocity of the vehicle. The effectiveness of the EDWL approach has been demonstrated by Chen and Wu (2010).

Rice formula

With the simulated deterministic load effects, the statistical parameters can be estimated by the tail fittings. The Rice formula (Rice 1945) was chosen in the present study to evaluate both the extreme traffic load effect and the probability of exceedance in the bridge lifetime. The principle of the Rice formula is shown in **Figs. 2.** In practice, the influence lines of long-span bridges are long enough, and the critical traffic loadings are mostly consistent with intensive vehicle use. Thus, the load effects can be assumed to be a Gaussian random process (Ditlevsen 1994). In addition, interval-based growth in traffic loading evidently satisfies the stationary assumption. Based on the above assumptions, the mean level-crossing rate $v(x)$ under the condition of a threshold l and a reference period is expressed as follows(Rice 1945):

$$v(x) = \frac{\dot{\sigma}}{2\pi\sigma}\exp\left[-\frac{(x-m)^2}{2\sigma^2}\right] = \frac{1}{R_t} \tag{2}$$

where, x is the traffic load effect, m and σ are the mean value and standard deviation of the load effect, respectively, and $\dot{\sigma}$ is the standard deviation of the derivative of the load effect. In general, the level-crossing rate can be expressed by a normalized rate indicated as fitted histograms versus the summation of truncated remaining histograms. The critical step of using the Rice level crossing theory for extrapolation is to determine the optimal starting point, indicated as $x_{0,opt}$, and the optimal number of class intervals, indicated as N_{opt} (Beck and Melchers 2004). For these determinations, the conventional approach is to utilize the Kolmogorov-Smirnov (K-S) statistics recommended by Cremona (2001) to check the

confidence level of the predefined starting point and number of class intervals. Eventually, the statistical extrapolation can be evaluated by the derivation of Eq. (2) considering a return period R_t.

Note that the extrapolated value x based on the level-crossing rate can also be defined as the value exceeded with a probability in a reference period. Therefore, the cumulative distribution function (CDF) of the maximum load effects can be written as follows:

$$F_{\max}(x,T) = 1 - a = 1 - \left[1 - \exp\left(-\frac{T}{R_t}\right)\right] = \exp\left\{-Tv_0 \exp\left[-\frac{(x-m)^2}{2\sigma^2}\right]\right\} \quad (3)$$

where, T is a general time period related to a reference period T_{ref}, i.e., a 100-year lifetime of a bridge in the present study, and a is a probability of exceedance, i.e., approximately 10% between T_{ref}=100 years and R_t = 1000 years. It is clear that the CDF can be estimated easily given the level-crossing function as shown in Eq. (3) for a stationary process. It is worth noting that these equations can only be used for stationary traffic loads without considering traffic growth. The growing traffic case is shown in next section.

Methodology for evaluating maximum load effects considering interval traffic growth

Traffic growth leads to a nonstationary density of vehicles on the bridge, which directly affects the maximum traffic load effects. An interval traffic growth model is utilized in the present study to divide the lifetime traffic loads into several intervals, each of which can be assumed to be non-growing and stationary. An improved Rice formula for combining the interval level-crossing models is presented in a detailed framework.

Interval traffic growth model

In general, the traffic volume grows continually over a given period. Such steady growth is usually defined as an annual growth rate (AGR) that is compounded between two years. Since

185 the traffic density over the bridge lifetime is nonstationary, the continual growth model is
186 inappropriate for use in the load effect extrapolation. However, the traffic volume can be
187 assumed to be stationary over short periods, such as one or two years. This short period is
188 defined as an interval in this study.

189 An example of the interval traffic growth is shown in **Figs. 3**, where the curve is the
190 volume of average daily truck traffic (ADTT) representing the assumed traffic growth and the
191 histograms are the volumes of the ADTT in the 10-year interval. It is obvious that the traffic
192 volume is constant during a given interval period rather than growing with the curve. The
193 advantage of the interval growth model is that Rice's formula can be applied to each interval.
194 The shortcomings of the interval growth model are that the result is only an estimate and that
195 its accuracy mostly depends on the number of intervals. Obviously, an increase in the
196 intervals improves the accuracy of the result but will also lead to additional computational
197 effects.

198 ***Improved Rice extrapolation account for interval traffic growth***

199 As mentioned before, the Rice formula, as shown in Eqs. (4) and (5), cannot be directly used
200 for traffic load effects under growing traffic load conditions because the traffic density is
201 nonstationary over the bridge lifetime. However, this formula is effective for individual time
202 intervals, as shown in Fig. 3(a). The question then becomes how to combine these individual
203 interval probability models to extrapolate the maximum value over a specified return period.
204 On the basis of related research conducted by Caprani et al. (2008) and Zhou et al. (2016),
205 this study utilizes a series system as shown in Fig. 3(b), to combine the intervals. Therefore,
206 the CDF of the maximum lifetime value can be estimated by multiplying each interval CDF,
207 which can be evaluated via Eq. (3), by T, which is equal to the interval period. Assuming that
208 the T_{ref} can be divided into N_{int} intervals, the lifetime CDF can be estimated using the interval
209 CDF products:

$$F_{\max}^{G}(x,T)=\prod_{i}^{N_{\text{int}}}F_{\max,i}(x,T_{\text{int}})=\exp\left\{-\sum_{i=1}^{N_{\text{int}}}T_{\text{int}}v_{0,i}\exp\left[-\frac{(x-m_i)^2}{2\sigma_i^2}\right]\right\} \quad (4)$$

where, $F_{\max}^{G}(x,T)$ is the maximum traffic load effect of a bridge in a reference period T considering traffic growth, N_{int} is the number of intervals, $T_{\text{int}}=T/N_{int}$ is the interval period, $F_{\max,i}(x,T)$ is the CDF of the maximum traffic load effects in the ith interval, and $v_{0,i}$ m_i and σ_i are the mean crossing rate, the mean value and the standard deviation of the load effects in the ith interval, respectively. Thus, the maximum load effects in a return period can be estimated based on the system CDF as shown in Eq. (4) and the general form of the CDF as shown in Eq. (3), written as

$$R_t=\frac{-T_{ref}}{\ln\left[F_{\max}^{G}(x,T_{ref})\right]} \quad (5)$$

where, each maximum load effect corresponds to a return period.

Herein, the critical steps of combining the interval traffic load effects for the extrapolation are as follows: (a) estimating the CDF of the traffic load effects in each interval based on Eq. (3); (b) combining the interval CDFs in a series system to formulate the actual CDF via Eq. (4); and (c) computing the return periods with respect to the maximum load effects via Eq. (5). The maximum load effect can also be interpolated from Gumbel probability paper.

In addition to the maximum extrapolation, the Rice formula can also estimate the probability of the maximum load effect exceeding a predefined limit over a reference period in terms of the probability of exceedance. A formulation of the probability of exceedance is written as follows:

$$p(z,t)\cong 1-F_{\max}(z,T_{ref}) \quad (6)$$

where, z is a predefined threshold for the traffic load effect, and $F_{max}(z,T_{ref})$ denotes the CDF of the maximum lifetime load effect at the limit z. This equation provides an approach for the

quantification of the probability of traffic load effects exceeding a limit.

A computational framework for extrapolating the maximum load effect of long-span bridges

Based on the interval traffic growth model and the improved Rice formula, a computational framework is presented for evaluating the maximum load effects of long-span bridges using WIM measurements. The flowchart of the computational framework is shown in **Fig. 4**. The entire procedure outlined in the flowchart is mainly composed of three categories: traffic load simulation, the load effect computation, and the probabilistic extrapolation. The procedures associated with the categories are described below.

The first module depicted in **Fig. 4** is the traffic load simulation based on recorded WIM data. With available WIM data, filtering procedures should be conducted to exclude invalid data and to select effective data that contribute to the maximum traffic load effect. In the present study, lightweight cars were removed from the recorded data because most of the critical loading scenarios usually involve dense traffic flows with a high proportion of heavy trucks. The statistical parameters of the traffic flow can be divided into two groups (O'Connor and OBrien, 2005): (a) those modeling the individual vehicle feature at small scales (i.e., the vehicle configuration, the gross vehicle weight, the vehicle spacing and the driving speed); and (b) those modeling the traffic feature at large scales (i.e., proportions of vehicle types and traffic volume). The most critical parameter is the vehicle spacing, defined as the space between two vehicles in the same driving lane. The vehicle spacing is a unique and critical factor for the traffic flow simulation on long-span bridges and is usually measured by the headway, which is time variant depending on the traffic density (OBrien and Enright 2012). The extreme traffic load effects are mostly induced by dense traffic flows with small vehicle spacings. Therefore, the PDF of the vehicle spacing in dense traffic flows is an important factor impacting the maximum traffic loading on a long-span bridge.

In general, traffic loads on a bridge can be simulated with a mathematical model in the time domain or in the space domain. A stochastic traffic flow is one of these mathematical models composed of individual vehicles formulated with statistical parameters. However, there is a problem with utilizing numerous daily traffic flows to conduct probabilistic and dynamic analyses because the step-by-step integration of the VBI system solution is extremely time consuming. Note that the purpose of using the daily traffic flow load model is to probabilistically model extreme traffic load effects. The maximum value is affected by the upper tail of the load effects produced by critical traffic loading scenarios. Therefore, critical traffic loading scenarios identified in a daily stochastic traffic flow can be utilized for the daily maxima simulation. The principle of identifying the critical traffic loading scenario is related to the static influence line analysis for determining the maximum load effects in the daily stochastic traffic flow. Based on this assumption, a step-by-step search strategy is adopted to identify the critical loading scenario. These procedures are as follows: (1) generating the stochastic traffic flows via MCS and the statistics of the WIM data; (2) specifying the effective range of the loading scenario on the bridge according to the bridge length; (3) moving the predefined range forward along the simulated daily stochastic traffic flows to calculate the static traffic load effect; (4) identifying the maximum load effect and the corresponding loading scenario; and (5) repeating steps (3) and (4) for the remaining daily traffic flows.

The second module is the traffic load effect computation. Two special factors are considered in this module: the VBI and the traffic growth. For the VBI, the dynamic vehicle load of the bridge under the critical loading scenario can be evaluated using the EDWL approach with the consideration of the RRC. The result is a time history that is then used for counting the number of level crossings. For the traffic growth, the interval traffic growth model is used to simulate traffic growth with an assumed AGR. The daily maxima in each

interval are estimated using the static influence lines.

The third module is the probabilistic extrapolation. The first step is to count the number of level crossings based on the estimated traffic load history or the interval daily maxima. The level-crossing rate as shown in Fig. 2(b), can be fitted to the histograms of the number of crossings. Then, the maximum traffic load effect over a return period can be extrapolated based on the Rice formula in Eq. (3) or the interval model in Eq. (4). Finally, the probability of exceedance of the predefined limit can be evaluated from the CDF of the maximum value.

Obviously, there are some key points in the proposed method. Firstly, a higher number of traffic intervals will lead to a more accurate extrapolation but will also lead to more computations. Additionally, because the actual traffic volume in each traffic interval will grow instead of being constant as assumed in the proposed approach, the extrapolated value will be slightly underestimated. In addition, the consideration of lightweight cars should be further developed.

Verification examples

Two numerical examples, including an individual GVW extrapolation and a deflection extrapolation of an idealized long-span bridge, are presented to verify the effectiveness of the interval traffic growth model.

Individual GVW extrapolation

A numerical example from OBrien et al. (2014) is presented here to verify the effectiveness of the interval traffic growth model. In this example, the block length is 1 day, the total lifetime is 25,000 days, the truck weights follow a normal distribution of $W_i \sim N(50,5)$ in tons, and the initial traffic volume is 1000 trucks per day. The objective of this numerical study is to extrapolate the maximum individual GVW over a bridge lifetime considering the daily traffic volume growth rate of 0.016% (an average AGR of 4.1%). OBrien et al. (2014) used a day-

by-day growth model to simulate the traffic growth, but the present study adopted a 10-year time interval. The GEV fitting utilized the entire 100-year daily maxima, while the Rice fitting utilized the 10-year 30% upper daily maxima. The following discussion focuses on the accuracy of the extrapolation, as the computational efficiency is the same.

Fig. 5(a) shows the annual crossing rates of the 1st, 5th and 10th interval periods fitted to histograms simulated by the daily maxima over 10 years. The mean value of the crossing rate apparently moves to the right hand side, and the mean level-crossing rate shows a slight decrease. **Fig. 5(b)** plots the maxima and fittings on Gumbel probability paper, where the 100-year daily maxima are shown as point symbols, the GEV fitting are shown as dash lines, and the Rice fittings are shown as solid lines. For the case of non-growing traffic, both the GEV and Rice extrapolations are in agreement with the value (77.50 t) provided by Obrien et al. (2014). However, for the case of growing traffic, the Rice extrapolation more accurately fits the reference value (80.60 t). Note that the exact value (78.842 t) for the case of non-growing traffic computed by the normal distribution of GVW to the power of 1000 is larger than the extrapolated value. This phenomenon can be explained by the fact that the convergence of a normal distribution to a Gumbel distribution is extremely slow and both the Rice and GEV extrapolations are underestimated.

The following inferences can be obtained from the numerical results: (a) the nonstationarity of the extreme distribution of the GVWs demonstrated by the level-crossing curves moving to the left side at higher intervals because the higher traffic volume increases the daily maxima and the number of higher-level crossings; (b) both the GEV and Rice fittings fit the daily maxima fairly well for the non-growing traffic condition since the GVW is stationary over the reference period; (c) the GEV fitting deviates from the tail of the daily maxima due to the nonstationarity of the traffic volume during the bridge lifetime; and (d) the Rice fitting is close to the tail, as the nonstationarity of the growing traffic has been captured

by the proposed method utilizing an interval traffic growth model. This example demonstrates the effectiveness of the proposed interval model for extrapolating a maximum individual GVW considering traffic volume growth.

Deflection extrapolation of an idealized long-span bridge

Since the objective is to apply the proposed method to long-span bridges, a second numerical example is presented to extrapolate the deflection of an idealized long-span bridge associated with the first example. This bridge and the traffic pattern are shown in **Fig. 6**, in which the vehicle spacing follows a normal distribution of S_i~N(100, 10) in meters, and the other parameters are the same as those in the first example. The objective of this example is to extrapolate the maximum deflection of the bridge over a 1000-year return period. The AGR is supposed to be between 0 and 1%.

The interval period is 2,500 days (effective working days in 10 years), and the lifetime includes 10 intervals. Step-by-step simulations based on the influence lines of the bridge were conducted to evaluate the daily maxima. Three typical annual crossing rates are shown in **Fig. 7(a)**. The crossing rate apparently moves to the right side and has a strong nonstationarity. The numerical results and a return period line are plotted in **Fig. 7(b)**. It is observed from the daily maxima that (a) the simulated daily maxima for the case of the no-growth model form a nearly straight line when plotted on the Gumbel probability paper; and (b) the daily maxima for the case of growing traffic model move to the left and form a curve when plotted on Gumbel probability paper. In addition, it is observed from the fittings that (a) for the case of non-growing traffic, the GEV and Rice fittings to the full data or the interval data are both well suited for extrapolating; (b) for the case of growing traffic, the GEV and Rice interval models yield better extrapolaitons than those of the GEV and Rice full data models; and (c) even though the Rice full data model has a relatively better extrapolation due to the optimal starting point, the interval growth model provides a much better extrapolation.

These phenomena can be explained by the following inferences. First, when considering traffic growth, the probability density of the traffic load effects is time-variant and will move to the higher-value side. The time-variant probability density violates the IID assumption, resulting in worse fitting via the general GEV distribution or Rice formula. Second, the Rice interval fitting is better for providing the extrapolation from the starting point of the final interval (105 mm in this example). Finally, the interval models provide better fittings for the higher-value data rather than the lower-value data. This pattern may be due to an insufficient number of intervals, as shown in **Fig. 3(b)** to capture a higher probability of exceedance.

Case study

A suspension bridge and its WIM data are utilized to demonstrate the effectiveness of the proposed computational framework. The dynamic characteristics and traffic growth are considered in order to investigate their influences on the probabilistic extrapolation.

Weigh-in-motion measurements of a suspension bridge

Nanxi Yangtze River Bridge is a long-span highway suspension bridge in Sichuan, China. A pavement WIM system composed of scales or pressure sensors embedded into the road pavement was installed on the bridge. More details of the bridge and the WIM measurements can be found in Liu et al. (2015) and Lu et al. (2016). A filtering process was conducted to identify and to remove invalid records, where the vehicles with the GVW less than 3 t were removed. An overview of the filtered WIM data is summarized in **Table 1**. The maximum overload rate was about 200% over the GVW limit (55 t) in China for a 6-axle truck (MOCAT 2004). A dense traffic flow composed of such extremely overloaded trucks is literally a hazard to the safety of long-span bridges.

Based on the WIM data and the assumption of stochastic traffic flow, the trucks were classified into 6 categories indicated as V1 ~ V6, where V1 denotes 2-axle light trucks and

V2 ~ V6 denote 2- to 6-axle trucks. The hourly traffic volume per lane was analyzed as shown in **Fig. 8(a)**. The hourly traffic volumes of the busy traffic period between 9:00 and 19:00 were utilized for statistical analysis of the truck spacing. The probability density of the truck spacing is accurately fitted by a lognormal distribution function (LNDF) as shown in **Fig. 8(b)**.

It is worth mentioning that the vehicle spacing in terms of traffic density is a significant factor impacting the traffic load effects on medium- to long-span bridges. This study ignores the effect of lightweight cars on the bridge defection computation by removing lightweight cars from the database. Therefore, the truck spacing in this study denotes the gap between two following trucks in a traffic lane, which is different from the vehicle spacing, which is defined as the vehicle gap between vehicles in the actual traffic stream. The effective truck spacing between two trucks (rather than the actual vehicle spacing) was utilized in the present study. The truck spacing makes sense in the context of probabilistic domain because the PDF of the truck spacing was fitted to the actual WIM data. Although the truck spacing does not represent an actual traffic state, the PDF has captured the statistical characteristics of the trucks in the actual traffic flows.

Extreme deflection considering dynamic traffic loads

As the first task, the commercial program ANSYS was utilized to construct the bridge finite element (FE) model shown in **Fig. 9**. In the FE model, the stiffening steel box girders and the concrete pylons were modeled using beam elements, and the hangers and the cables were modeled using link elements. Additionaly, the bridge tower elements and the cable elements were separated and the top joints were connected by a set of coupled degrees of freedom. This study takes into consideration the pre-tension forces in the main cable and hangers as well as the self-weight of the bridge, which are essential parameters in the mechanical analysis of a suspension bridge. The pre-tension forces and dead loads were considered in the FE model in

406 the first time step, followed by modal and static analysis. The value of the pre-tension forces
407 and the secondary dead loads were initially determined by the design values and were
408 subsequently updated to bring the structural modal characteristics in agreement with the
409 measured data. It is worth noting that the structural stiffness accounting for the pre-tension
410 forces and the dead load was considered but that the load effect due to the pre-tension forces
411 and the dead load was excluded because the present study concentrated only on the traffic
412 load effect. It is acknowledged that long-span bridges are geometrically nonlinear, especially
413 under heavy traffic loads. The present study, however, is limited to a linear analysis as a first
414 step implementing the improved stochastic analysis. The advancement of the improved
415 stochastic analysis can be extended to the nonlinear case but the computational efficiency
416 should be further developed.

417 **Table 2** summarizes the first 5 fundamental mode characteristics of the FE model. In
418 total, 50 mode frequencies and mode shapes were used in the mode superposition. The vehicle
419 physical properties in this case study were adopted from Yin et al. (2011). The RRC in this
420 study was defined based on the International Organization for Standardization (1995). The
421 RRCs for classifications of "Good", "Average", and "Poor" are 32×10^{-6}, 128×10^{-6}, and
422 512×10^{-6}, respectively. The RRC coefficients were simulated via inverse Fourier
423 transformation approach in the time domain.

424 As the second task, the dynamic traffic load effects at the critical points of the bridge
425 were simulated. Initially, conditions involving a 2-axle truck with a GVW of 10 t, a driving
426 speed v of 20 m/s, and an RRC of "Good" were considered to determine the static and
427 dynamic deflections of the bridge girders. The static analysis was conducted by considering a
428 moving concentrated force F of 100 kN, and the dynamic analysis was conducted via the
429 EDWL approach considering vehicle-bridge interaction. **Fig. 10** shows the mean vertical
430 deflections of the three potential points versus the truck loading position on the bridge. It is

observed that the most critical point is the $L/4$ (quarter-span) point. The maximum deflections due to static and dynamic loads are 0.029 m and 0.032 m, respectively. Therefore, the subsequent investigation focuses on the quarter-point of the bridge.

Subsequently, the critical traffic loading scenarios were identified from the simulated daily stochastic traffic flows. The procedures are as follows: firstly, the vehicle type was randomly sampled according to the proportion of each vehicle type; secondly, the vehicle weight and the driving lane of the vehicle was determined according to their probability densities; thirdly, the vehicle spacing of the following vehicle was determined; finally, the above procedures were repeated to generate a traffic flow model. The stochastic traffic flows were first put into the static influence line to conduct a static analysis. The static deflection was analyzed to identify the critical traffic loading scenario that was then utilized for dynamic analysis. Only a critical loading scenario in each 10 h stochastic traffic flow is necessary for the extreme traffic load effect analysis because the dynamic analysis of a 10 h daily traffic load is time consuming. An illustration of the process for generating the critical loading scenario on a 4-lane bidirectional bridge is shown in **Figs. 11**, where traffic lanes 1 and 2 are in the same direction, and traffic lanes of 3 and 4 are in the opposite direction. A daily maximum deflection was identified from the static deflection histories in **Fig. 11(a)**, and the corresponding critical traffic loading scenario was extracted from the daily stochastic traffic load as shown in **Fig. 11(b)**. Obviously, the critical loading scenario is a small part (0.1%) of the daily traffic flow. As a result, the time-consuming computation due to the step-by-step integration can be greatly reduced by utilizing the critical traffic loading scenario rather than the entire stochastic daily traffic flows. Therefore, the static analysis can identify the critical loading scenarios for dynamic analysis, thereby improving the efficiency of the dynamic computation of numerous traffic flows.

In total, 1,000 days of traffic flows were simulated via Monte-Carlo simulation and the probability density models of the current WIM traffic data. These critical traffic streams are free flowing with a constant velocity v=20 m/s. Each time-variant concentrated force was computed via the EDWL approach in modal superposition, and was then put into ANSYS to conduct the traffic load effect analysis. Fig 12(a) shows two traffic loading scenarios for better understanding the dynamic and static deflection histories shown in Fig. 12(b). A reference line in Fig. 12(b) counts the number of level crossings at the deflection level a=-0.667 m, where terms N^i_{static} and $N^i_{dynamic}$ are the number of crossings for the static and dynamic histories, respectively. Note that the deflection level was utilized to count the number of crossings, whereas the deflection threshold was utilized to evaluate the probability of exceedance. It is observed, from **Fig. 12(b),** that the dynamic histories fluctuate around the static histories. This makes the numbers of level crossings different. The number of dynamic crossings is always higher than that of static crossings. This numerical result shows the advantage of the Rice formula in capturing the dynamic effects.

Based on the Rice formula, the down-crossing histograms and estimated crossing rates of the dynamic and static histories were estimated, as shown in **Fig. 13**, where x_0 is the optimal starting point estimated by the K-S test. It is observed that the dynamic effect has a higher crossing rate, while the mean value and the standard derivation have negligible differences. With the fitted level-crossing models, extrapolations of the maximum deflection were estimated. **Fig. 14** shows the results of the static and dynamic extrapolations for a 1000-year return period.

As shown in **Fig. 14**, the maximum deflections over a return period of 1000 years are 1.445 m, 1.458 m, 1.464 m and 1.475 m for the static results for “Good”, “Average” and “Poor” roughness conditions, respectively. It is observed that the lifetime dynamic ratio, i.e., the ratio between dynamic and static extrapolations, for the poor road roughness condition is

1.021. Therefore, although poorer RRCs lead to a larger number of level crossings, its influence on the maximum traffic load effect extrapolation of a long-span bridge appeas to be negligible.

Lifetime maximum deflection assessment considering interval traffic growth

The European commission predicts a sustainable annual growth ratio of truck traffic volume between 1.5% and 2% (European Commission 2008). Therefore, in the present study, the linear AGR of the traffic volume was set to 0, 1%, 2%, and 3%, and the traffic featured free-flowing conditions. The 100-year lifetime of the bridge was divided into 10 intervals in which the traffic volume was stationary and non-growing. In total, 1000 days of daily maxima for each interval were utilized to estimate the level-crossing model as shown in **Fig. 15**. It is observed that the level-crossing rate is constant for the non-growing traffic model, while the level-crossing curves apparently move to the left with traffic growth, with a higher traffic growth rate leading to a larger shift. The traffic growth for long-span bridges not only results in a large traffic volume but also leads to a higher traffic density on the bridge. Increases in both of these parameters lead to a rapid growth of the extrapolation of the maximum deflection. This phenomenon is in agreement with the numerical results presented in the verification examples.

Based on the estimated level-crossing models, the extrapolation of maximum deflection over a 1, 000-year return period was estimated based on Eq. (6). **Fig. 16** plots the extrapolations in the bridge lifetime accounting for the traffic growth. It is obvious that the traffic growth leads to a rapid growth of the maximum deflection. As a result, an *AGR* of 3% increases to the extrapolation of the lifetime maximum deflection by 18%.

The probability of exceedance of a deflection limit is a serviceability criterion for a bridge under traffic loading. The exceedance criterion was defined as the maximum deflection of the quarter-point of the bridge girder crossing the deflection limit specified in native/local

specifications. Therefore, it is important to define a threshold deflection for the prototype bridge under traffic loading. As mentioned in the introduction, different design codes have different limits, such as $L/350$ and $L/800$ for long-span bridges and simply supported bridges, respectively (AASHTO, 2015). In the present study, the deflection limit was set to $L/400$ according to China's code (MOCAT 2007).

The probability assessment of the maximum deflections is shown in **Figs. 17**. **Fig. 17(a)** shows estimated CDFs of the maximum deflections in the lifetime estimated and plotted on Gamble probability paper, and **Fig. 17(b)** shows the probabilities of exceedance of the deflection limit over the 100-year period. The *x*-axis values at the cross point in **Fig. 17(a)** are similar to the values shown in **Fig. 16**. Therefore, the CDF and the extrapolations are in agreement. The probabilities of exceedance for an *x*-axis value of 2.05 m in **Fig. 17(b)** are 1.1×10^{-11}, 2.0×10^{-9}, 4.9×10^{-8} and 2.7×10^{-7} for traffic growth raties of 0, 1%, 2% and 3%, respectively.

It is inferred that traffic growth has a significant influence on the probability of exceedance. This influence is greater for a lower limit, but weaker for a higher limit. In addition, an increase in the traffic growth rate leads to a higher rate of increase in the probability of exceedance. This phenomenon can be explained by the fact that traffic growth not only leads to a larger daily maxima of an individual truck weight but also increases the traffic density on the bridge. Therefore, a reasonable traffic growth model is critical for evaluating the maximum traffic load effect over the lifetimes of a bridge.

Conclusions

This study presents a methodology for statistical extrapolation of traffic load effects over the lifetime of long-span bridges. Advancements have been made in several challenging areas related to realistically addressing vehicle-bridge interactions, actual traffic patterns and traffic growth. The actual traffic pattern was modeled via stochastic traffic flows simulated based on

530 weigh-in-motion measurements. The continuously growing traffic loads were considered as a
531 series system composed of interval traffic loads. The nonstationarity of the growing traffic
532 load was captured in this model. The methodology was verified by two numerical examples
533 and was subsequently applied to the lifetime maximum deflection extrapolation of a
534 suspension bridge. The following conclusions have been drawn from the numerical studies.
535 (1) Traffic volume growth leads to a time-variant level-crossing rate, which violates the IID
536 in the GEV extrapolation theory. Therefore, the conventional model deviates from tail of
537 the maxima plotted on Gumbel probability paper and provides poor extrapolations.
538 However, the interval traffic growth model in series has the ability to capture the
539 nonstationalry of growing traffic load effects. The interval fitting of the GEV or Rice
540 extrapolations represents the tail fairly well and provides relatively accurate extrapolations.
541 (2) Not only does traffic growth results in a higher daily maximum GVW, but it also
542 increases the traffic density on the bridge, which is the main reason leading to the
543 significant increase of in lifetime traffic load effect.
544 (3) The vehicle-bridge coupled vibration under worse road roughness condition leads to more
545 level crossings of the bridge deflection, but it does not significantly impact the mean value
546 and the standard deviation of the level-crossing rate. As a result, the lifetime dynamic
547 assessment ratio is less than 2.1%.
548 (4) For the site-specific traffic condition of the suspension bridge, the annual traffic growth
549 rate of 3% leads to an 18% increase in the extrapolated maximum deflection for within a
550 1000-year return period.
551 (5) The traffic growth has a significant influence on the probability of exceedance of the
552 deflection limit. Such influence is more significant for a lower threshold deflection level,
553 but it is minor for a higher limit. In addition, a higher traffic growth rate leads to a rapid
554 increase in the probability of exceedance.

Although the proposed methodology was applied to the lifetime maximum deflection extrapolation of a suspension bridge, it can also be extended to extrapolate of the maximum bending moment, the maximum cable force, and the longitudinal displacement of other long-span bridges. The findings from the presented study provide a basis for extension in the following direction. Firstly, as an alternative approach of MCS, cellular automaton and Markov chain sampling can be utilized to simulate the microscale behaviour of vehicles, such as changes in the vehicle spacing on the bridge. Secondly, improvements can be made through focusing on congested traffic conditions rather than on free-flow traffic conditions and adjustments in the model since congested traffic conditions were found to be more critical to the maximum deflection. Thirdly, the approximation of the traffic load by removing the highly proportioned lightweight cars from the WIM database was found to be potentially critical since it may result in the distortion of the vehicle spacing in the simulated stochastic traffic flow. Finally, nonlinear stochastic analysis should be considered in the proposed approach, but the computational efficiency associated with the demanding nonlinear calculations is a key problem.

Acknowledgements

This work was supported by the National Basic Research Program (973 program) of China (Grant 2015CB057705), the National Science Foundation of China (Grant 51378081), and the Key Laboratory of Bridge Engineering Safety Control by Department of Education in Changsha University of Science and Technology (Grant 16KD03).

References

AASHTO. (2015). *LRFD bridge design specifications*, 6th Ed., Washington, DC.

ANSYS [Computer software]. ANSYS, Canonsburg, PA

Beck, A.T., Melchers, R. (2004). “On the ensemble crossing rate approach to time variant reliability analysis of uncertain structures.” *Probabilist. Eng. Mech.*, 19(1): 9-19.

580 Caprani, C., OBrien, E., and McLachlan, G. (2008). "Characteristic traffic load effects from a
581 mixture of loading events on short to medium span bridges." *Struct. Saf.*, 30(5), 394-404.
582 Caprani, C. C., González, A., Rattigan, P. H., & OBrien, E. J. (2012). "Assessment dynamic
583 ratio for traffic loading on highway bridges." *Struct. Infrastruct. E.*, 8(3), 295-304.
584 Caprani, C., OBrien, E., and Lipari, A. (2016). "Long-span bridge traffic loading based on
585 multi-lane traffic micro-simulation." *Eng. Struct.*, 115, 207-219.
586 Cai, C. S., and Chen, S. R. (2004). "Framework of vehicle–bridge–wind dynamic analysis." *J.*
587 *Wind. Eng. Ind. Aero dyn.*, 92(7–8), 579–607.
588 Chen, S., and Cai, C. (2007). "Equivalent wheel load approach for slender cable-stayed bridge
589 fatigue assessment under traffic and wind: Feasibility study." *J. Bridge Eng.*,
590 10.1061/(ASCE)1084-0702(2007)12:6(755), 755-764.
591 Chen, S. R., & Wu, J. (2010). "Dynamic performance simulation of long-span bridge under
592 combined loads of stochastic traffic and wind." *J. Bridge Eng.*,
593 10.1061/(ASCE)BE.1943-5592.0000078, 219-230.
594 Cremona, C. (2001). "Optimal extrapolation of traffic load effects." *Struct. Saf.*, 23(1): 31-46.
595 Ditlevsen, O. (1994). Traffic loads on large bridges modeled as white-noise fields. *J. Bridge*
596 *Eng.*, 10.1061/(ASCE)0733-9399(1994)120:4(681), 681-694
597 Deng, L., Wang, W., & Yu, Y. (2016). "State-of-the-art review on the causes and mechanisms
598 of bridge collapse." *J. Perform. Constr. Facil*, (10.1061/(ASCE)CF.1943-5509.0000731)
599 ECS (European Committee for Standardization). (2005). Eurocode 3: Design of steel
600 structures: general rules and rules for buildings." *EN 1993–1-1*, Brussels, Belgium.
601 European Commission. Directorate General for Energy and Transport, 2008. European
602 Energy and Transport. Trends for 2030. Update 2007.
603 Fu, G., and You J. (2009). "Truck loads and bridge capacity evaluation in China." *J. Bridge*
604 *Eng.*, 10.1061/(ASCE)BE.1943-5592.0000006, 327-335.

605 Enright, B., Carey, C., and Caprani, C. C. (2013). "Microsimulation evaluation of Eurocode
606 load model for American long-span bridges." *J. Bridge Eng.*, 10.1061/(ASCE)BE.1943-
607 5592.0000209, 812-819.
608 Enright, B., and OBrien, E.J. (2013). "Monte Carlo simulation of extreme traffic loading on
609 short and medium span bridges." *Struct Infrastruct. E.* 9(12): 1267-1282.
610 Han, W., Wu, J., Cai, C. S., and Chen, S. (2014). "Characteristics and dynamic impact of
611 overloaded extra heavy trucks on typical highway bridges." *J. Bridge Eng.*,
612 10.1061/(ASCE)BE.1943-5592.0000666, 05014011.
613 ISO. (1995). Mechanical vibration-road surface profiles-reporting of measured data, *ISO*
614 *8069: (E)*, Geneva, Switzerland.
615 Kwon, O. S., Kim, E., & Orton, S. (2010). "Calibration of live-load factor in LRFD bridge
616 design specifications based on state-specific traffic environments." *J. Bridge Eng.*,
617 10.1061/(ASCE)BE.1943-5592.0000209, 812-819.
618 Liu, Y., Deng, Y., and Cai, C. S. (2015). Deflection monitoring and assessment for a
619 suspension bridge using a connected pipe system: a case study in China. *Struct. Control*
620 *Health.*, 22(12), 1408-1425.
621 Lu N., Noori M., and Liu Y. (2016). "Fatigue reliability assessment of welded steel bridge
622 decks under stochastic truck loads via machine learning." *J. Bridge Eng*. (DOI:
623 10.1061/(ASCE)BE.1943-5592.0000982).
624 MOCAT, (2004). "Limits of dimensions, axle load and masses for road vehicles." *GB 1589-*
625 *2004*, Beijing, China.
626 MOCAT, (2007). "Specifications for design of highway cable-stayed bridge." *JTG/T D65-01*,
627 Beijing, China.
628 Nowak, A. S. (1995). "Calibration of LRFD bridge code." *J. Struct. Eng.*,
629 10.1061/(ASCE)0733-9445(1995)121:8(1245), 1245-1251.

630 OBrien, E., Cantero, D., Enright, B., & Gonzalez, A. (2010). “Characteristic dynamic
631 increment for extreme traffic loading events on short and medium span highway bridges.”
632 *Eng. Struct.* 32: 3827-3835.
633 OBrien, E., and Enright, B. (2011). “Modeling same-direction two-lane traffic for bridge
634 loading.” *Struct. Saf.*, *33*(4), 296-304.
635 OBrien, E., and Enright, B. (2012). “Using weigh-in-motion data to determine aggressiveness
636 of traffic for bridge loading.” *J. Bridge Eng.*, 10.1061/(ASCE)BE.1943-5592.0000368,
637 232-239.
638 OBrien, E., Hayrapetova, A., and Walsh, C. (2012). “The use of micro-simulation for
639 congested traffic load modeling of medium-and long-span bridges.” *Struct. Infrastruct.*
640 *E.*, 8(3), 269-276.
641 OBrien E.J., Bordallo-Ruiz A., and Enright B. (2014). “Lifetime maximum load effects on
642 short-span bridges subject to growing traffic volumes.” *Struct. Saf.*, 50: 113-122.
643 OBrien, E., Lipari, A., and Caprani, C. (2015a). “Micro-simulation of single-lane traffic to
644 identify critical loading conditions for long-span bridges.” *Eng. Struct.*, *94*, 137-148.
645 OBrien E., Schmidt F., Hajializadeh D., Zhou, X., Enright, B., Caprani, C.C. Wilson, S., and
646 Sheils, E. (2015b). “A review of probabilistic methods of assessment of load effects in
647 bridges.” *Struct. Saf.*, 53: 44-56.
648 O'Connor, A., and OBrien, E. J. (2005). “Traffic load modelling and factors influencing the
649 accuracy of predicted extremes.” *Can. J. Civil Eng.*, 32(1), 270-278.
650 Rice, S.O. (1945). Mathematical analysis of random noise. *The Bell System Technical*
651 *Journal*, 24(1), 46-156.
652 Ruan, X., Zhou, J., and Caprani, C. (2016). Safety assessment of the antisliding between the
653 main cable and middle saddle of a three-pylon suspension bridge considering traffic load
654 modeling. *J. Bridge Eng.*, 10.1061/(ASCE)BE.1943-5592.0000927 , 04016069.

Wang, L., Zhang X., Zhang J., Yi, J., and Liu, Y. (2017). "Simplified Model for Corrosion-Induced Bond Degradation between Steel Strand and Concrete." *J. Mater. Civil Eng.*, 10.1061/(ASCE)MT.1943-5533.0001784, 04016257.

Yin, X., Fang, Z., and Cai, C. (2011). "Lateral vibration of high-pier bridges under moving vehicular loads." *J. Bridge Eng.*, 10.1061/(ASCE)BE.1943-5592.0000170, 400-412.

Zhu, S., Levinson, D., Liu, H., and Harder K. (2010). "The traffic and behavioral effects of the I-35W Mississippi River bridge collapse." *Transport Res A-Pol*, 44(10): 771-784.

Zhou, Y. and Chen, S. (2014). "Dynamic simulation of a long-span bridge-traffic system subjected to combined service and extreme loads." *J. Struct. Eng.*, 10.1061/(ASCE)ST.1943-541X.0001188, 04014215.

Zhou, Y. and Chen, S. (2015). "Fully coupled driving safety analysis of moving traffic on long-span bridges subjected to crosswind", *J. Wind Eng. Indu. Aerod.*, 143, 1-18.

Zhou, Y. and Chen, S. (2016). "Vehicle ride comfort analysis from whole-body vibration on long-span bridges subjected to crosswind", *J. Wind Eng. Indu. Aerod.*, 155, 126-140.

Zhou, X., Schmidt, F., Toutlemonde, F., and Jacob, B. (2016). "A mixture peaks over threshold approach for predicting extreme bridge traffic load effects." *Probabilist. Eng. Mech.*, 43, 121-131.

Zhang, N., and Xia, H. (2013). "Dynamic analysis of coupled vehicle–bridge system based on inter-system iteration method." *Comput. Struct.*, 114, 26-34.

Tables Captions

Table 1. Overview of the filtered WIM measurements

Table 2. The first five order mode frequencies of the suspension bridge

679 **Table 1.** Overview of the filtered WIM measurements

Items	Values
Time period	May 1, 2013 to April 30, 2015
Number of recording days	729
Total number of effective trucks	1, 563, 921
Maximum GVW (t)	164
Number of overloaded trucks	12, 252

680

681 **Table 2.** The first five order mode frequencies of the suspension bridge

Order	Mode frequency		Error (%)	Illustration
	FE model	Monitored data		
1	0.131	-	-	1st antisymmetric transversal bending
2	0.1781	0.1849	-3.68	1st antisymmetric vertical bending
3	0.2208	0.2492	-11.40	1st symmetric vertical bending
4	0.3106	0.3049	1.87	2st antisymmetric vertical bending
5	0.4074	0.3975	2.49	2st symmetric vertical bending

682

Figures Captions

708 CDFs plotted on Gamble paper; (b) probability of exceedance

Figure 1

Click here to download Figure Fig. 1.pdf

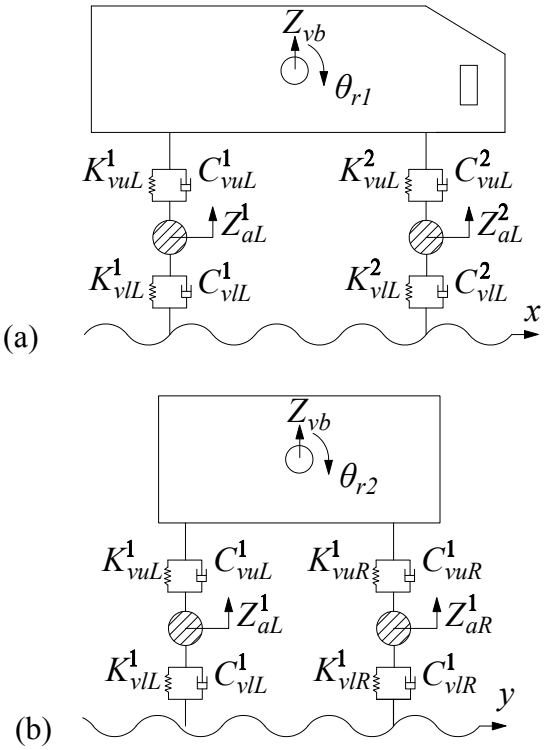

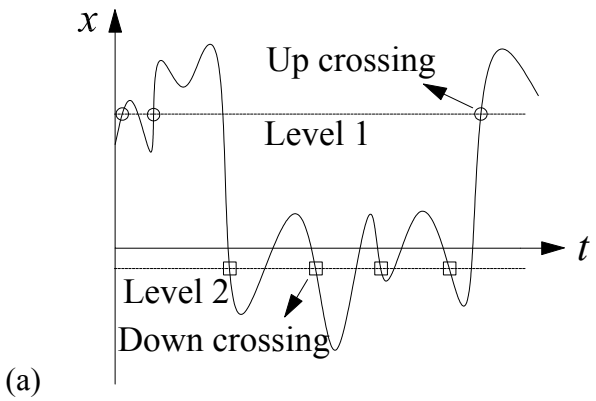

(a)

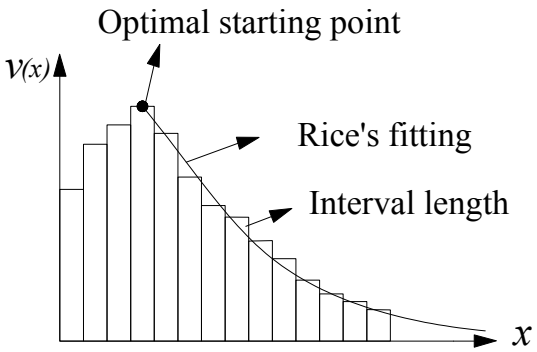

(b)

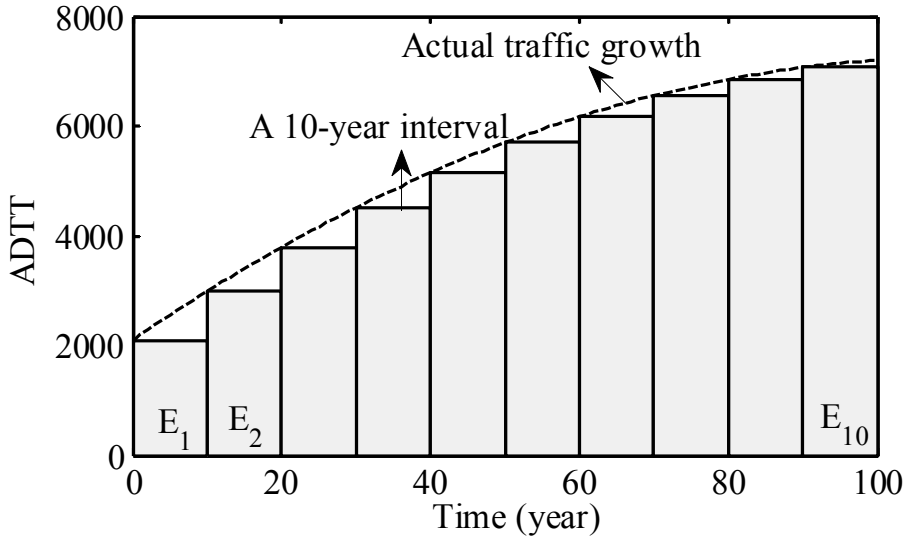

(a)

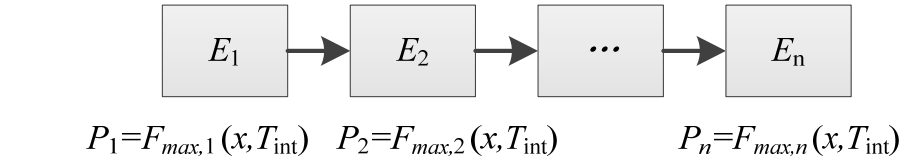

$P_1=F_{max,1}(x,T_{int})$ $P_2=F_{max,2}(x,T_{int})$ $P_n=F_{max,n}(x,T_{int})$

(b)

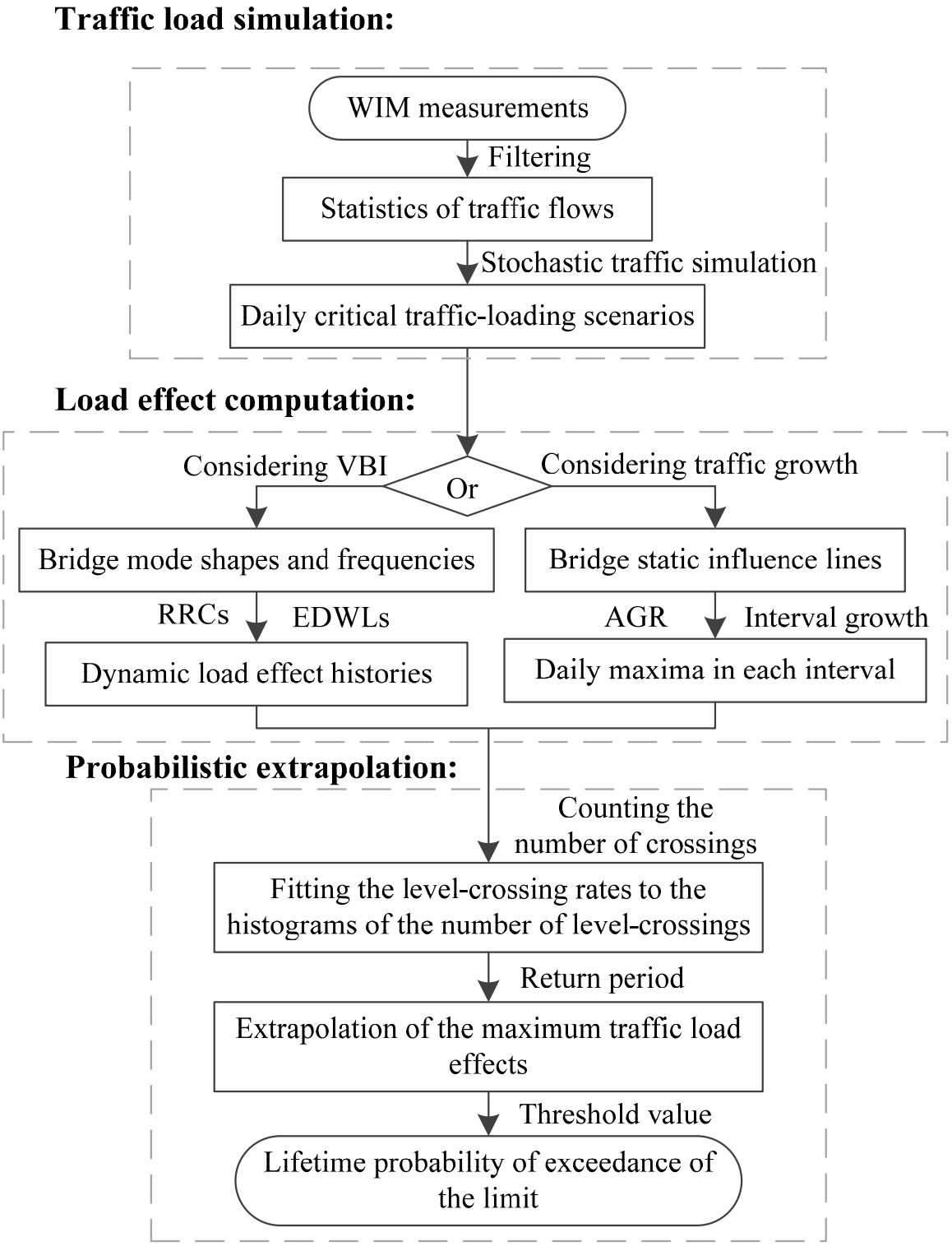

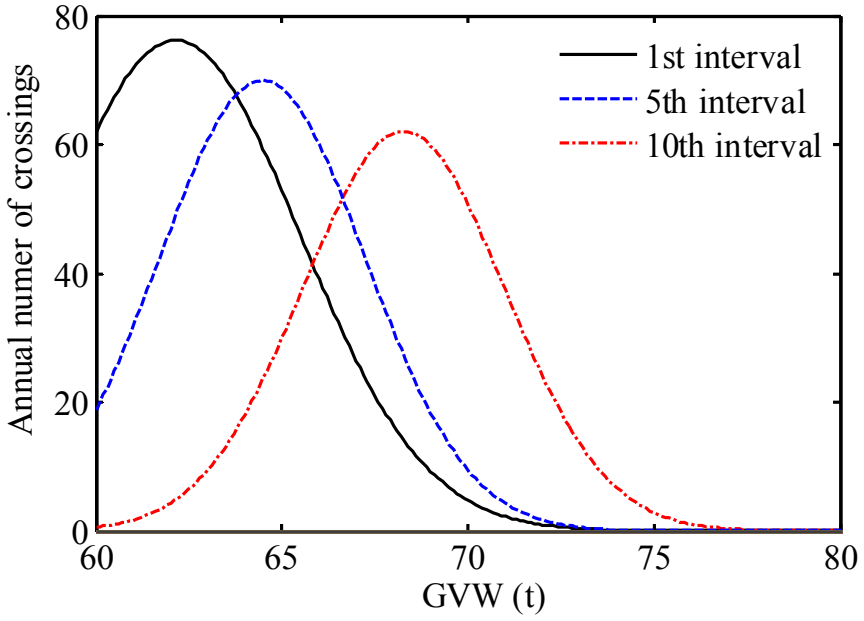

(a)

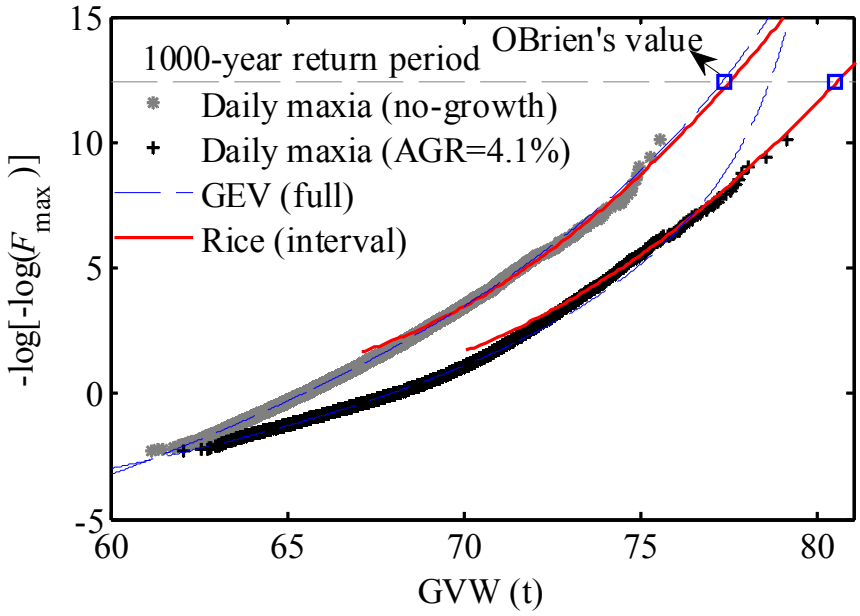

(b)

Figure 6 Click here to download Figure Fig. 6.pdf

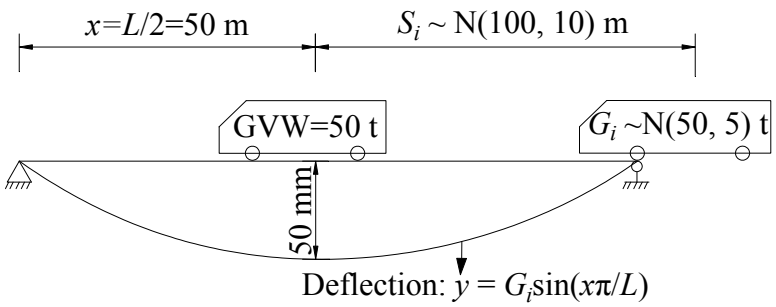

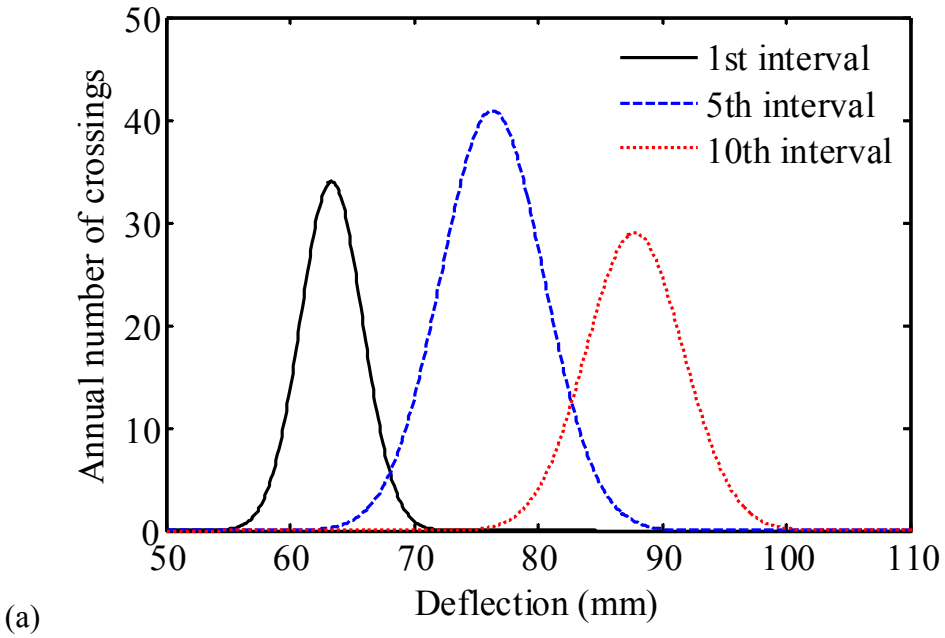

(a)

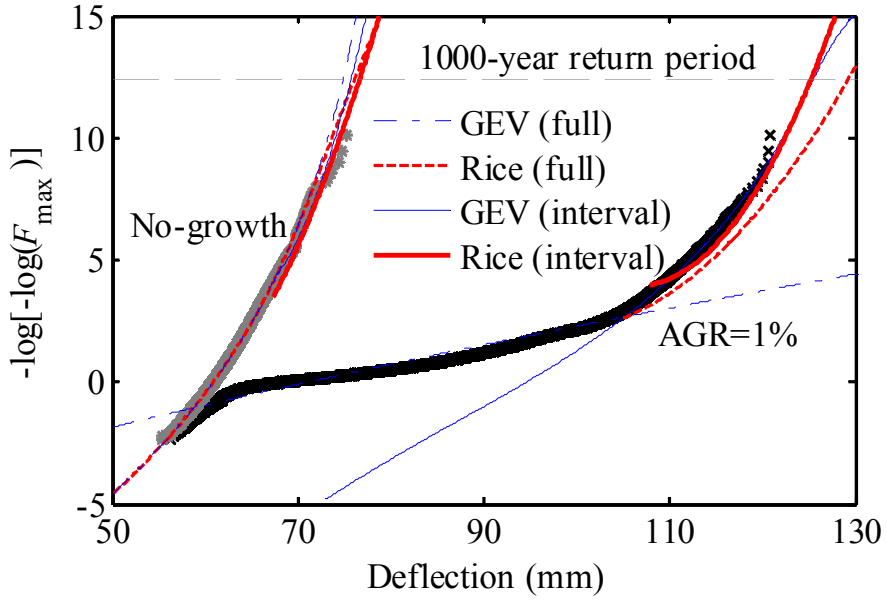

(b)

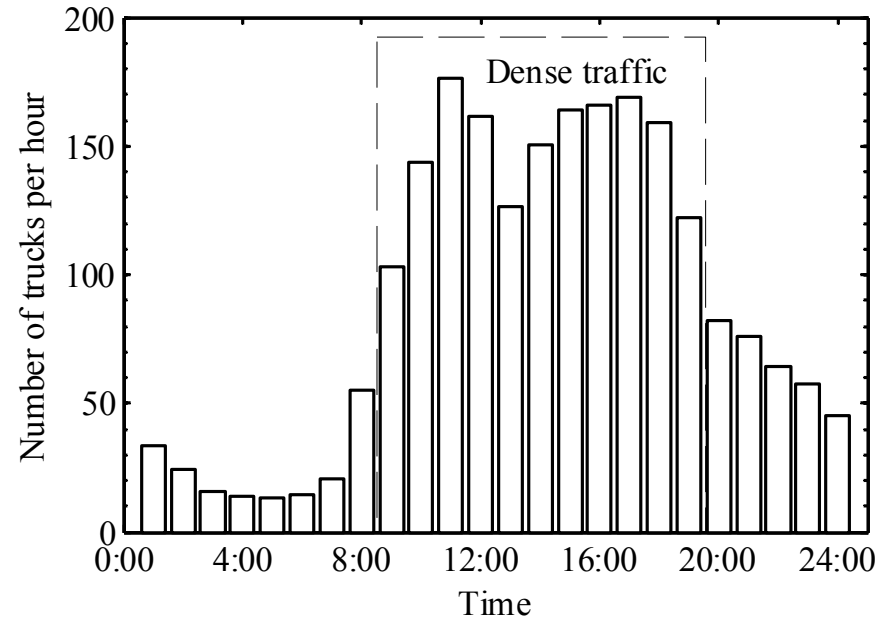

(a)

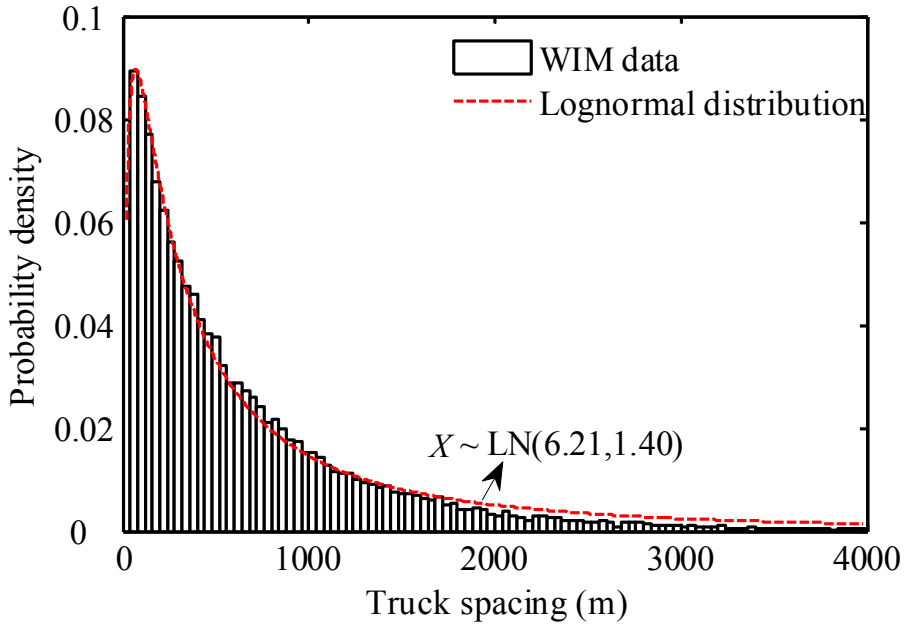

(b)

Figure 9

Click here to download Figure Fig. 9.pdf

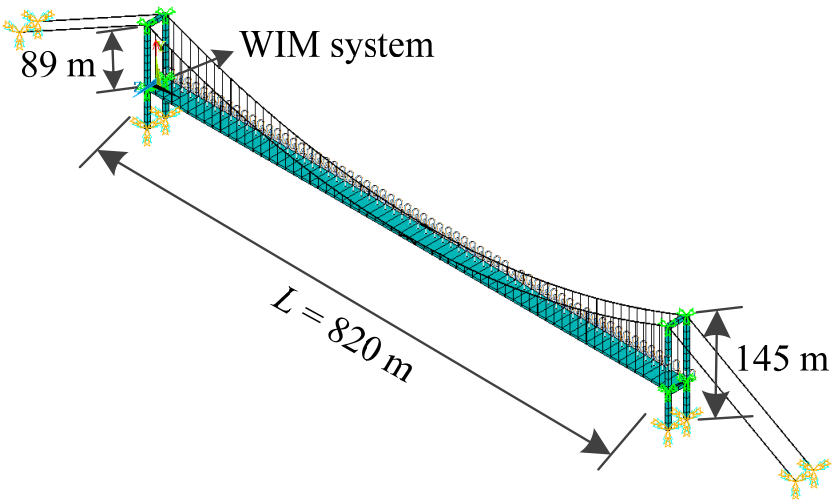

Figure 10

Click here to download Figure Fig. 10.pdf

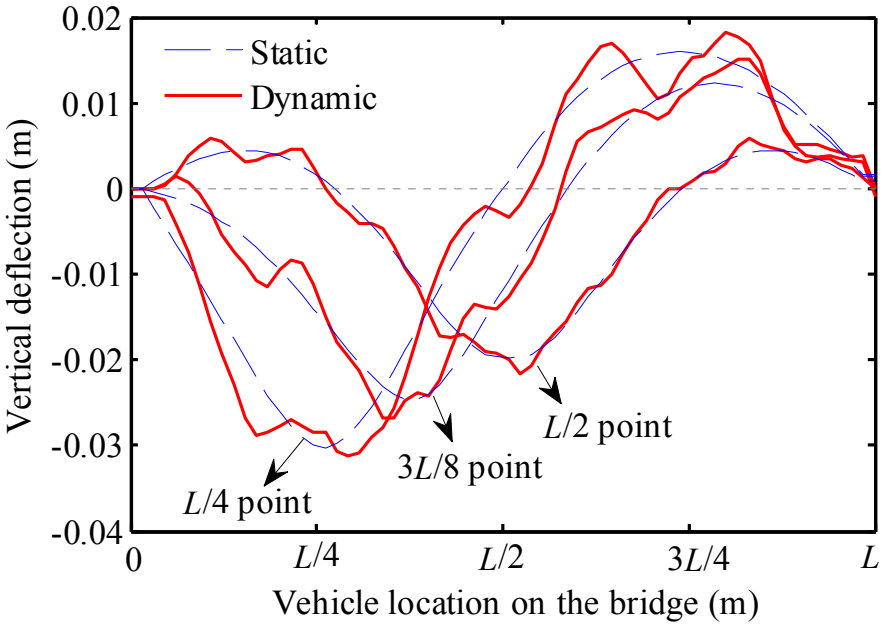

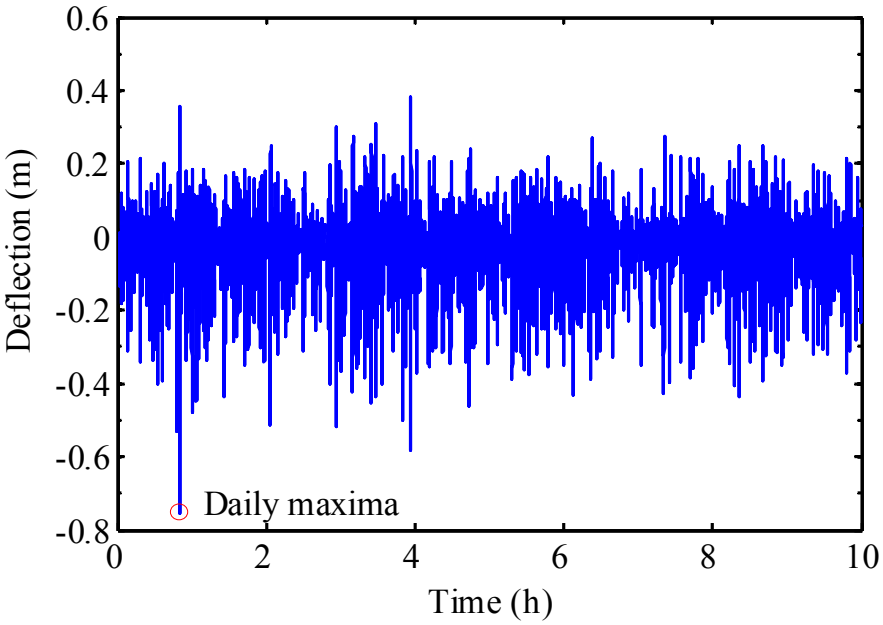
0.6
0.4
0.2
0
-0.2
-0.4
-0.6
-0.8
Deflection (m)
Daily maxima
0
2
4
6
8
10
Time (h)

(a)

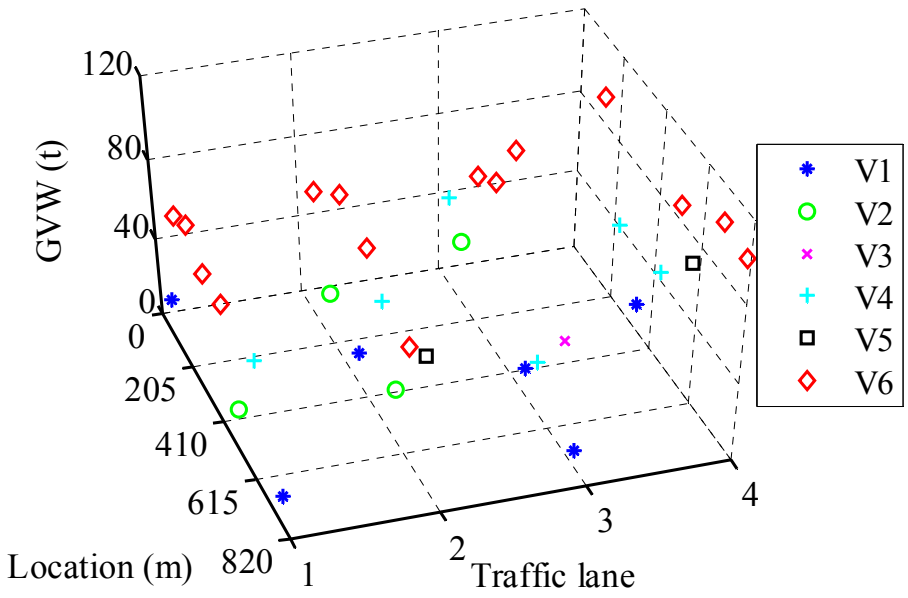
120
80
40
0
GVW (t)
0
205
410
615
820
Location (m)
1
2
3
4
Traffic lane
V1
V2
V3
V4
V5
V6

(b)

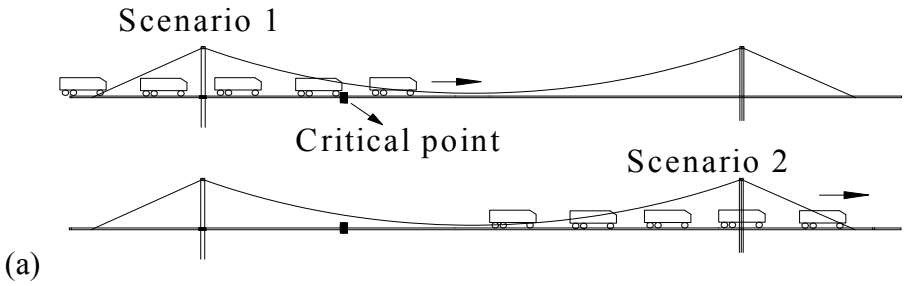

(a)

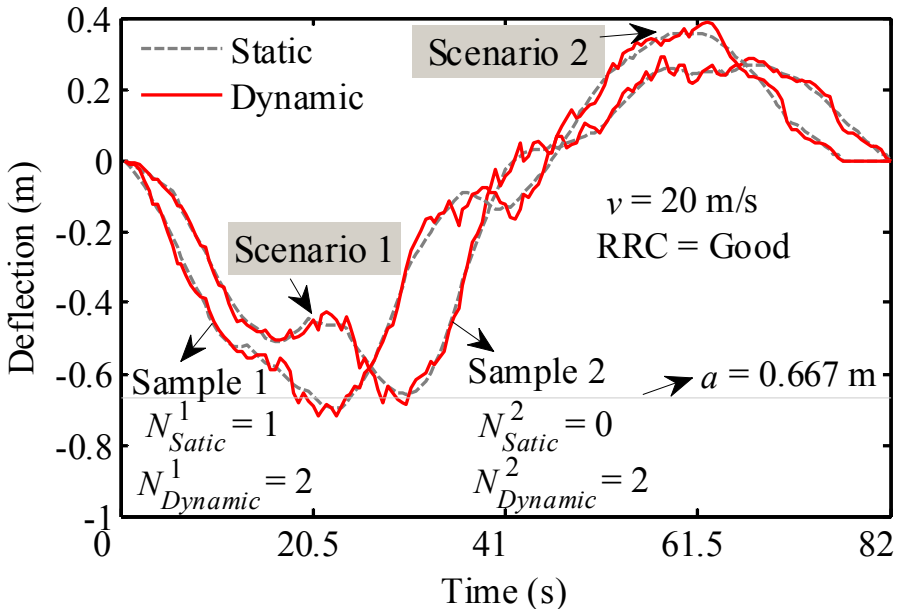

(b)

Figure 13

Click here to download Figure Fig. 13.pdf

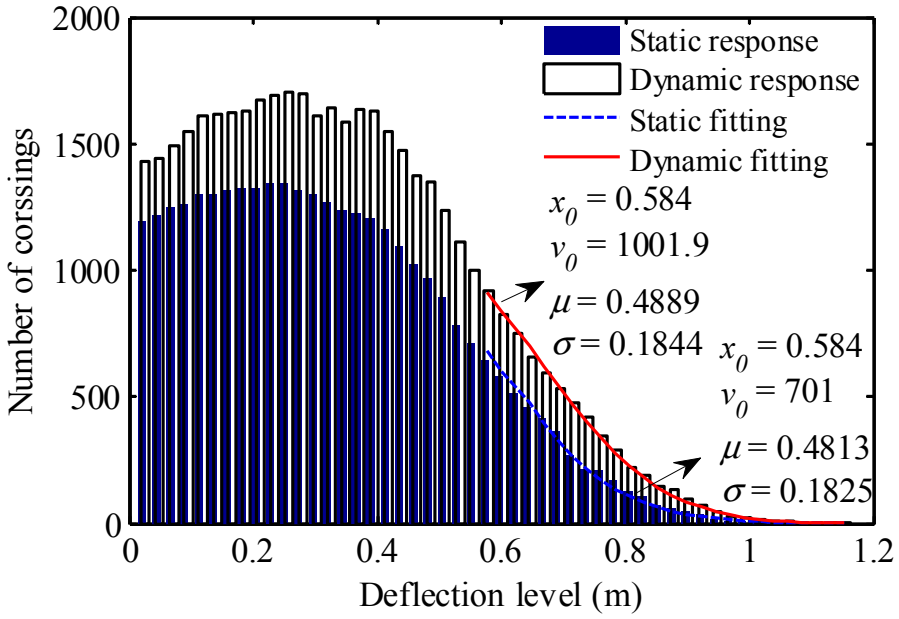

Figure 14

Click here to download Figure Fig. 14.pdf

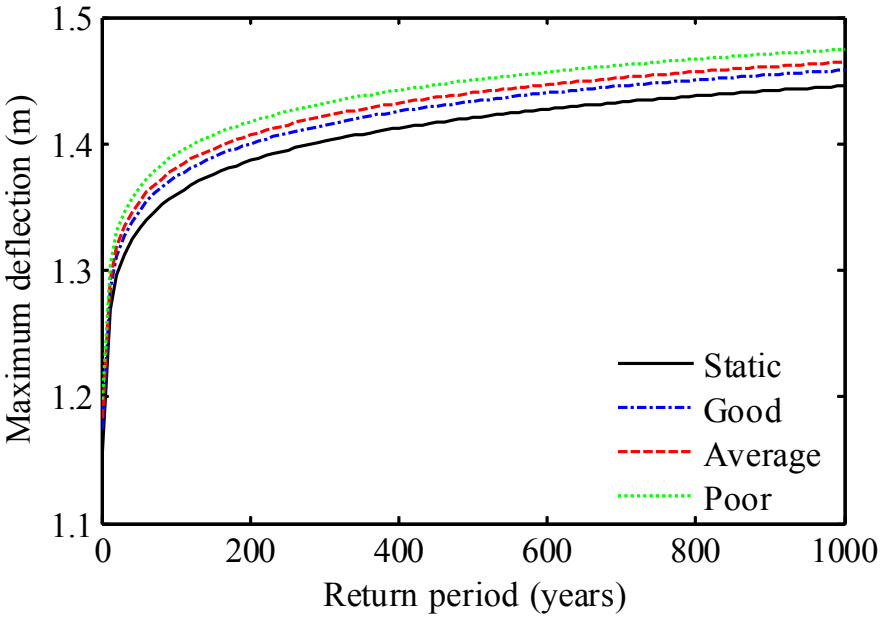

Figure 15

Click here to download Figure Fig. 15.pdf

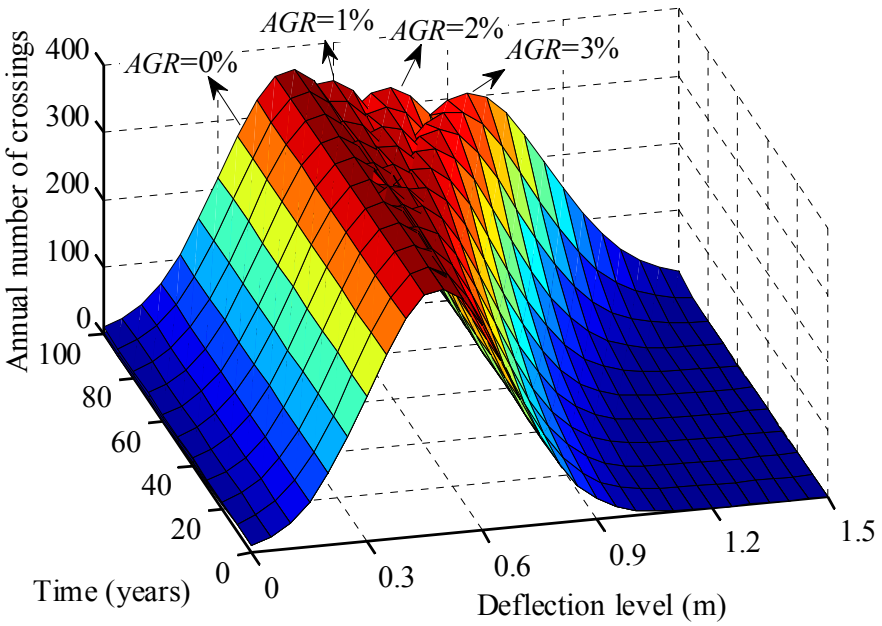

Figure 16

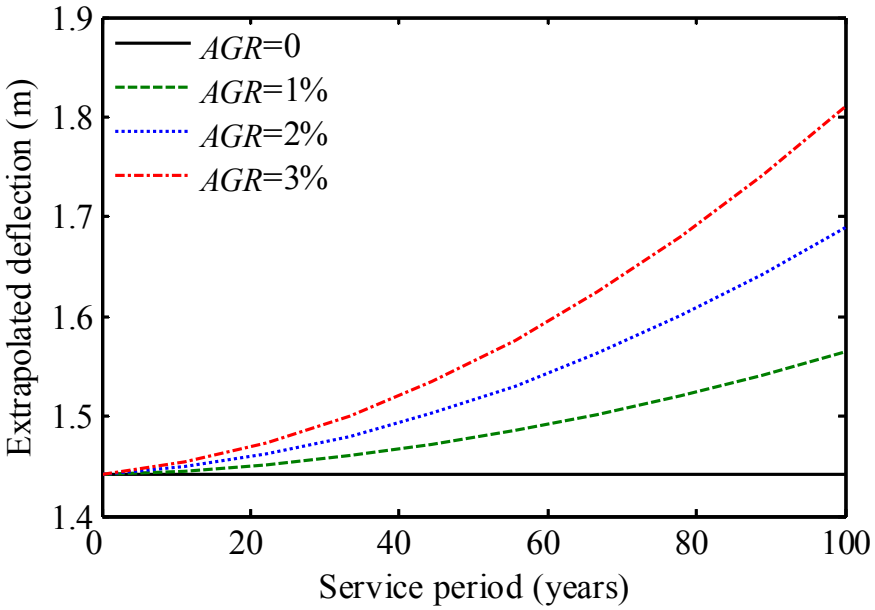

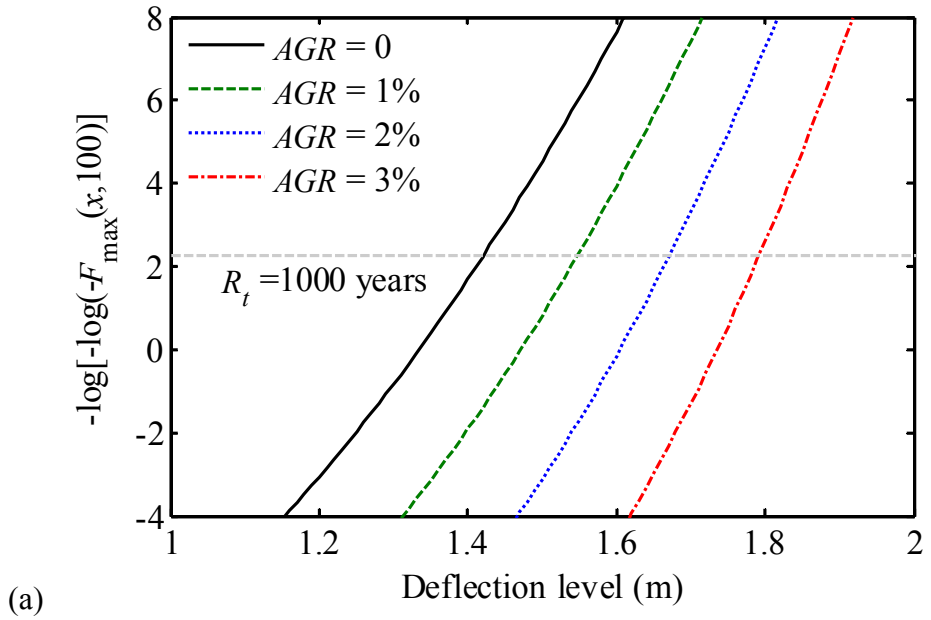

(a)

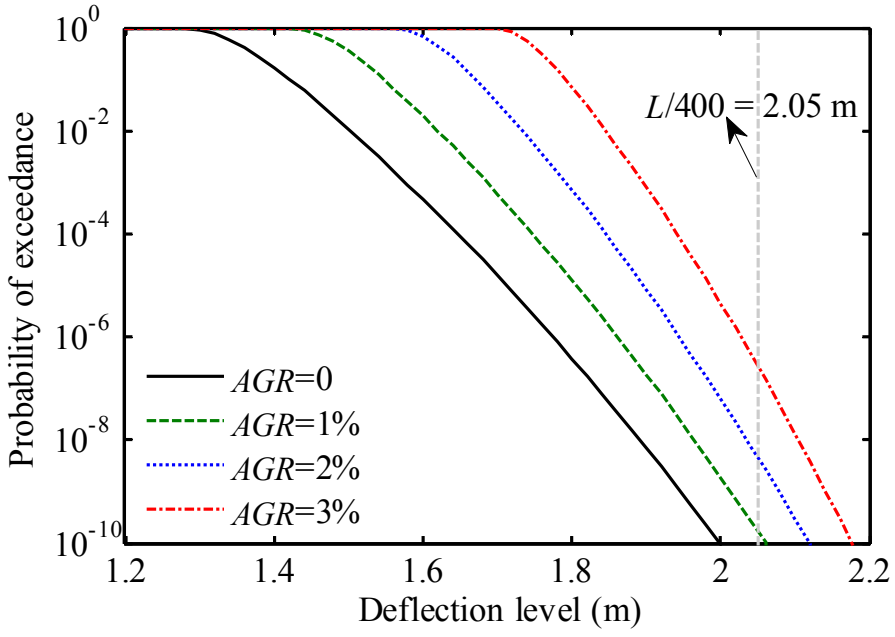

(b)